Jour. of the KGS, Vol. 20, No. 2. March 2004, pp. 125~130

Parameter Evaluation of a Smooth Elasto-plastic Cap Model

연속탄소성 캡 모델의 정수 산정

Seo, Young-Kyo[1] 서 영 교

요 지

본 논문에서는 수치적 구성방정식인 연속 탄소성 캡 모델의 정수추정에 관한 방법이 제시되었다. 캡 모델을 이용하여 실제 토질의 거동을 예측하기 위하여서는 캡 모델을 이루는 토질의 물성과 직접적으로 연관된 여덟 개의 정수가 결정되어야 한다. 이를 위하여 첫 번째로, Ottawa 모래를 사용하여 표준압밀시험기를 이용한 일축압축시험 및 배수삼축압축 시험이 토질거동의 실제기준값으로서 수행되었고, 두 번째로 탄소성 캡 수치해석모델의 반응을 실내실험값에 일치시키기 위하여 추정된 정수들을 사용한 수치실험이 수행되었다. 두 실험 간의 오차를 최소화 하기위하여 최적화 기법이 사용되었으며, 최적화 후 결정된 8개의 정수는 실내실험결과와 비교되었다. 특히, 수치적 삼축압축시험시 응력계산에 따른 수평변위 측정에 특별한 주의가 필요하다.

Abstract

In this paper, the method of parameter estimation of a mathematical constitutive model known as the smooth elasto-plastic cap model is studied. To predict the response of the real soil using this model, the eight parameters describing the constitutive equations have to be determined. First, experimental data are obtained from simple laboratory experiments such as one dimensional confined compression test in a consolidometer and drained triaxial compression test with the Ottawa sand for the reference value. Then, the numerical experiments are performed in the cap model with initial guessed parameters. The optimization method is utilized to fit the model response to experimental data by minimizing the error between the laboratory and numerical responses. Special attention is given to the parameter estimation procedure of numerical triaxial test due to the difficulty of the lateral strain measurements.

Keywords : Cap models, Elasto-plasticity, Optimization, Parameter estimation

1. Introduction

Once a mathematical constitutive law consistent with the physical behaviors is derived, it is necessary to identify and choose all significant parameters that are needed to define it. In this paper, the parameter estimation method of the elasto-plastic cap model (Seo, 2001) is studied.

Several methods for determining the unknown parameters have been presented in the literature. The standard curve fitting method (Desai and Siriwardane, 1984; Zaman et al., 1982) was used based on physical insight into the experimental data. Although this procedure provides a parameter fitting inspired by construction of the numerical model, it has some drawbacks: (1) a large amount of conventional experimental data is required;

1 Member, Full-Time Lecture, Div. of Ocean Development Engrg., Korea Maritime Univ. (yseo@hhu.ac.kr)

and (2) it is not possible to use some existing non-conventional experimental data. Gauss-Newton method (Matsui et al., 1994) and Marquardt-Lenvenberg method (Simo et al., 1998) were also reported based on optimization techniques. Gauss-Newton is simple and uses a limited amount of test data, however, there is a major drawback. The coefficient matrix of simultaneous equations can be singular or nearly singular which leads to numerical instabilities. In this case, if the objective function becomes completely insensitive to any of the design variables during the optimization iteration, the matrix will be rank deficient.

In this study, an alternative constrained optimization procedure which is using the existing optimization code such as IDESIGN (Arora et al., 1997) embedded SQP algorithm is utilized with limited test data. Using the commercial optimization program can avoid the complicated optimization coding procedure with numerical stabilities. In the simulation reported herein, two tests of simple laboratory experimental data, using the Ottawa sand for the reference value, are used to define the eight material parameters (α, θ, W, D, κ, H, λ and μ) that make up the cap model. This paper starts a brief review of the smooth cap model, then the detailed parameter estimation procedure will be explained as follows.

2. Description of the Cap Model

In this section, the basic constitutive equations of a smooth three surface cap model (Seo, 2001) are first summarized. Utilizing the assumption of small deformation, the strain tensor admits the additive elasto-plastic decomposition;

$$\varepsilon = \varepsilon^e + \varepsilon^p \tag{1}$$

where ε, ε^e and ε^p are the total, elastic, and plastic strain tensors, respectively. The elastic response of the material is assumed to be characterized by a constant isotropic tensor $C = K\,1\otimes 1 + 2\mu I_{dev}$ and the incremental stress response of the material is given by

$$\dot{\sigma} = C:(\dot{\varepsilon} - \dot{\varepsilon}^p) \tag{2}$$

where K is the bulk modulus of the soil and μ is the shear modulus. In a stress space, the elastic domain is bounded by three distinct yield surfaces which are functions of the two invariants $I_1 = tr(\sigma)$ and $||s||$, where s is the deviatoric part of the stress tensor σ(*i.e.* $s = I_{dev}:\sigma$). The three surfaces comprising the yield surface intersect in a smooth manner as shown in Fig. 1.

The form of the yield function, $f_m(\sigma, x)$ $(m = 1, 2, 3)$ is specified in terms of functions F_e, F_c and F_t which are respectively called the Drucker-Prager envelope function, the compression cap function, and the tension cap function. The mathematical forms are

$$f_1(\sigma, q) = ||\eta||^2 - F_e(I_1) \le 0 \tag{3}$$

$$f_2(\sigma, q, x) = ||\eta||^2 - F_c(I_1, x) \le 0 \tag{4}$$

$$f_3(\sigma, q) = ||\eta||^2 - F_t(I_1) \le 0 \tag{5}$$

where: $\eta = s - q$ and $||\eta||^2 = [\eta:\eta]^{1/2}$. As is customary s denotes the deviatoric stress, and q denotes a purely deviatoric back stress associated with kinematic hardening. The specific forms of F_e, F_c and F_t are defined here as

$$F_e(I_1) = \alpha - \theta I_1 \qquad I_1^C(x) \le I_1 \le I_1^T \tag{6}$$

$$F_c(I_1, x) = R^2(x) - (I_1 - x)^2 \qquad I_1 < I_1^C(x) \tag{7}$$

$$F_t(I_1) = R_T^2 - I_1^2 \qquad I_1 > I_1^T \tag{8}$$

In the preceding expressions, α and θ are basic material constants. Approximate translation from Mohr-Coulomb parameters to Drucker-Prager parameters has been provided, as for example in Chen and Saleeb(1982), as

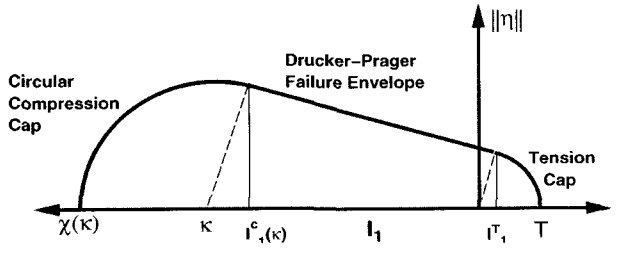

Fig. 1. Smooth, three-surface, two invariant yield functions for a cap model

$$\alpha = \frac{\sqrt{2}c}{(1+4/3\tan^2\phi)^{1/2}} \text{ and}$$

$$\theta = \frac{\sqrt{2}\tan\phi}{3(1+4/3\tan^2\phi)^{1/2}} \quad (9)$$

Whereas the entities I_1 and $I_1^C(\kappa)$ denote, respectively, a fixed delimiting point between the Drucker-Prager envelope and the tension cap, and the Drucker-Prager envelope and the compression cap. Specific expressions for these points are

$$I_1^T = \alpha\cos(\phi)\sin(\phi) \quad (10)$$

$$I_1^C = \kappa + R(\kappa)\sin(\phi) \quad (11)$$

where $\phi = \tan^{-1}(\theta)$. As the compression cap surface translates along the I_1 axis, the cap surface radius $R(\kappa)$ changes as a function of the cap parameter κ as follows

$$R(\kappa) = -\kappa\sin(\phi) + \alpha\cos(\phi) \quad (12)$$

The tension cap surface is circular. The center of tension cap resides at $I_1 = 0$, and the radius of the surface is a constant R_T which is expressed as

$$R_T = \alpha\cos(\phi) \quad (13)$$

The hardening law for this model derives from the fact that the volumetric crush curve (plastic volumetric strain ε_v^p versus I_1) is assumed to be an exponential of the form

$$\varepsilon_v^p = W[1-\exp\{DX(\kappa)\}] \quad (14)$$

Differentiating the equation with respect to κ allows us to obtain a variable tangent hardening modulus $h'(\kappa)$ for κ as follows

$$h'(\kappa) = \frac{d\kappa}{d\varepsilon_v^p} = \frac{\exp(-DX)}{WDX'} \quad (15)$$

where $X' = 1 - RF_e(\kappa)$; W represents the maximum possible plastic volumetric strain for the medium, with the reference state being the material's virgin unloaded state; and D^{-1} denotes the absolute value of I_1 at which $e^{-1}\cdot 100\%$ of the medium's original crushable porosity remains. This nonlinear hardening modulus $h'(\kappa)$ is used to provide a nonlinear incremental hardening law governing movement of the cap parameter

$$\dot{\kappa} = h'(\kappa)\,tr(\dot{\varepsilon}^p) \quad (16)$$

A purely deviatoric linear kinematic hardening law is employed with this model, the rate form of which is

$$\dot{q} = H I_{dev}\cdot\dot{\varepsilon}^p \quad (17)$$

where H is a constant plastic hardening modulus.

The flow rule for this model is associated, and since multiple surfaces are potentially active at any given instant, it takes Koiter's generalized form

$$\dot{\varepsilon}^p = \sum_m \dot{\gamma}^m \frac{\partial f_m}{\partial\sigma} \quad (18)$$

in the above expressions, α, θ, W, D, χ, H, λ, and μ are material parameters which characterize the smooth cap model considered here.

3. Optimization Problem

Sequential quadratic programming(SQP) method uses the Taylor series expansion to linearize a nonlinear optimization problem and linerarized subprogram transformed to a quadratic program. While this method uses the basic idea as the Gauss-Newton method, it treats the optimal fitting process as a least square constrained optimization problem. The constrains imposed on the optimization problem are in the sense of physically meaningful bounds. The formal statement of the optimization problem is

$$MIN\,J(b) \equiv \sum_{j=1}^{N}(u_j - z_j(b))^2 \quad \text{subjected to}$$

$$a_i \le b_i \le c_i;\quad i = 1 \text{ to } 8 \quad (19)$$

where N is number of observation; u_j is observed response from the laboratory experiments; z_j is response from constitutive model; j is j^{th} data point; b_i are design parameter vectors; a_i and c_i are lower and upper bounds of design variables. The constrains imposed on

the optimization problem emanate from physical restrictions placed on the cap parameters. For example, for a physically meaningful model, one should have $b_i > 0$. There exists a wide variety of algorithms to solve the above constrained optimizatiom poblems. To avoid implementing a such algorithms, the existing optimization code IDESIGN (Arora et al., 1997) was used here due to its robustness and generality. The sequential quadratic programming algorithms can be found in Arora (1989).

Since the magnitude of cap model parameters are vastly different in size, it is important to normalize the design variables for better performance of the optimization process. The normalized design variables b_i are defined as

$$b_i = \frac{x_i}{k_i} \tag{20}$$

where x_i are the i^{th} original design variables and k_i are their normalization factors. Thus, using appropriate k_i, the design variables can be forced to vary approximately between -1 to +1. The derivatives of an objective function $J(x_i)$ with respect to normalized variables b_i are given as

$$\frac{\partial J}{\partial b_i} = \frac{\partial J}{\partial x_i}\frac{\partial x_i}{\partial b_i} = \frac{\partial J}{\partial x_i} k_i \tag{21}$$

The optimal algorithm with the normalized design variables can be applied to any set of experimental data to obtain the optimal fit in a least square sense for the constitutive model under consideration.

4. Parameter Estimation and Results

In order to access the capability of smooth cap model in predicting response behavior of a real material, model parameters are needed to be estimated from laboratory experimental data. In this section parameter estimation procedure for one dimensional confined compression test and drained triaxial compression test with Ottawa sand are presented, followed by the numerical simulation results. Satisfactory agreements are achieved between experimental data and numerical model responses.

4.1 Estimation from One Dimensional Compression Test

For the uniaxial strain test conducted in the laboratory, the dry sand sample was loaded axially under stress controlled mode. The schematic diagram for the test is shown in Fig. 2.

A general procedure for the estimation of material parameters used by the constitutive model is as follows; 1) initial normalized design variables b_i are assumed within physically reasonable bounds; 2) the design variables were unscaled ($x_i = k_i \cdot b_i$) to calculate the response

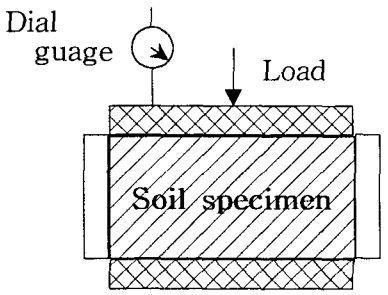

Fig. 2. Diagram of experimental uniaxial compression test

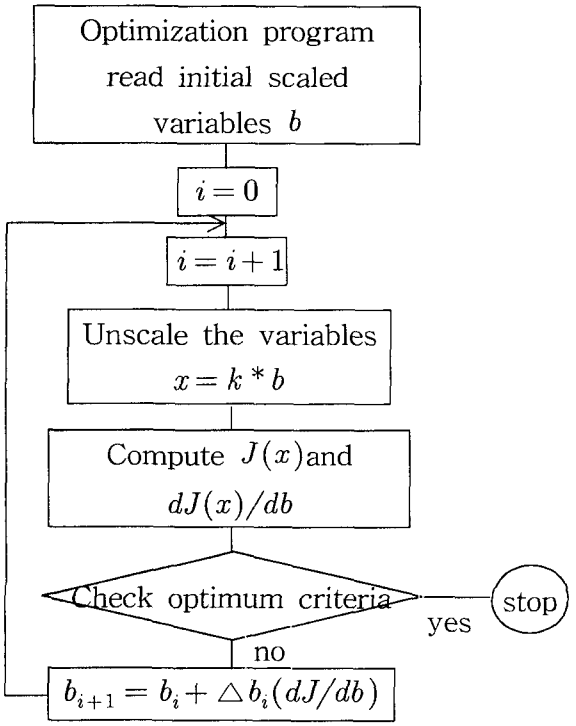

Fig. 3. Optimization algorithm

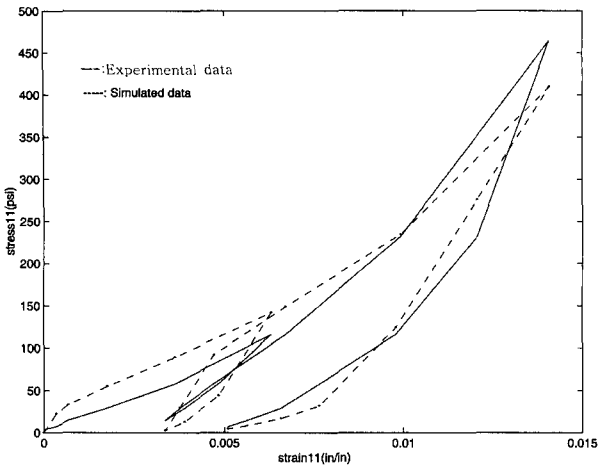

Fig. 4. Simulated results in uniaxial compression test

Table 1. Optimal value for Ottawa sand

Material Parameter (Upper and lower bound)	Uniaxial strain test (Optimal value)	Triaxial test (Optimal value)
$0 \le \lambda \le 10^{9} (kN/m^2)$	2.3719×10^{7}	2.3719×10^{7}
$0 \le \mu \le 10^{9} (kN/m^2)$	1.1101×10^{7}	1.1101×10^{7}
$0 \le \alpha \le 10^{5} (N/m^2)$	2.9717×10^{2}	3.6957×10^{2}
$0 \le \theta \le 0.5$	0.2727	0.2727
$0 \le W \le 0.1$	0.0157	0.0157
$0 \le D \le 10^{-3} (kN/m^2)^{-1}$	2.994×10^{-4}	2.994×10^{-4}
$-10^{5} \le x \le 0 (N/m^2)$	-100	-1000

from the constitutive model; 3) the objective function and the gradient were computed.

The estimation algorithm is shown in Fig. 3. A comparison between experimental and predicted curve is shown in Fig. 4. The values of the material parameters obtained in the estimation process and the boundary values used are summarized in Table 1.

4.2 Estimation from Drained Triaxial Compression Test

In the laboratory experimental test, a confining pressure (cp) is first applied, by using a fluid in the chamber. Once an equilibrium state of stresses was reached, the additional axial stress ($\triangle \sigma_1$) is then slowly increased while the drainage connected is opened. The increased axial stress causes shearing of the specimen. A diagram of triaxial test layout is shown in Fig. 5. This test features both stress and strain controlled aspects. In the first stage, which is stress controlled, a confining pressure is applied and the volumetric strain results. In the second stage the lateral stresses are maintained while the axial strain is applied.

In the numerical simulation for the parameter estimation for drained triaxial compression test, there need to be two steps. 1) **Pre-load step**: In this step, volumetric strain is applied with small increment to the constitutive model until the stresses reach designated confining pressure. 2) **Generating the triaxial data**: Since, a conventional triaxial test has difficulty in measuring the lateral strain increment, which are needed for the optimization input data, for given stress increment, numerical procedures, such as Newton-Raphson iteration method with line search, are used for generating the lateral strain($\varepsilon_1 = \varepsilon_2$). There might be several strain increment steps in the strain-stress curves.

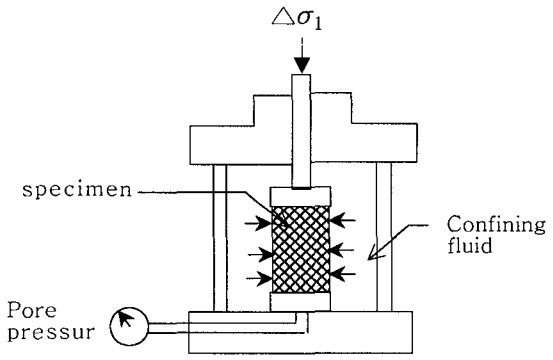

Fig. 5. Diagram of the experimental triaxial test layout

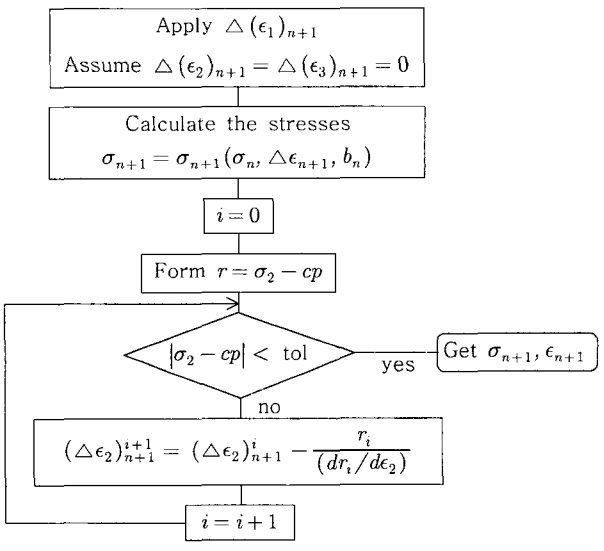

Fig. 6. Computational triaxial compression test algorithm

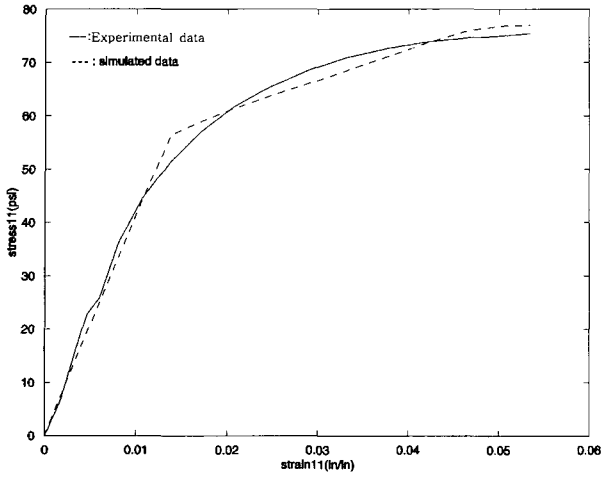

Fig. 7. Simulated results in triaxial compression test

At single increment strain step ($\triangle\varepsilon_{1(n+1)}$) with the assumption of $\triangle\varepsilon_{2(n+1)}=\triangle\varepsilon_{3(n+1)}=0$, we need to find $\sigma_{1(n+1)}$ and $\varepsilon_{2(n+1)}=\varepsilon_{3(n+1)}$ such that $\triangle\sigma_{2(n+1)}=\triangle\sigma_{3(n+1)}=0$. The complete algorithm is shown in Fig. 5. After the previous two steps are complete, the object function and the gradient of the objective function are computed for the optimization process (refer to Fig. 3). A comparison between experimental and predicted stress-strain curve is shown in Fig. 6. The values of the material parameters obtained in the estimation process and the boundary values used are summarized in Table 1.

5. Conclusion

The parameter estimation procedures for the soil model have been presented to identify the eight parameters of the smooth cap model using Ottawa sand. Experimental data are first obtained from uniaxial strain test and triaxial test which are considered to be representative of material response. Then, the numerical simulations with initially guessed values are performed until the model responses are matched with the experimental test results. Special attention is given to the parameter estimation procedure of numerical triaxial test due to the difficulty of the lateral strain measurements.

Acknowledgements

This work was supported by the Brain Busan 21 Project in 2003.

References

1. Arora, J. S (1989), Introduction to Optimal Design, McGraw-Hill Series.
2. Arora, J. S., Lin, T., Elwakeil, O., and Haung, M. (1997), "IDESIGN users' manual version 4.2", Optimal Design Laboratory, The Univ. of Iowa, Iowa City.
3. Chen, W.-F. and Saleeb, A. F. (1982), Constitutive Equations for Engineering Material, Vol. 1: Elasticity and Modeling, John-Wiley.
4. Desai, C. S. and Siriwardance, H. I. (1984), Constitutive laws for engineering materials, Prentice Hall, Englewood-Cliffs, NJ.
5. Matsui, K., Nishida, N, Dobashi, Y. and Ushioda, K. (1994), "An inverse method for estimation of termal properties of mass concrete", Transations of Japan Concrete Institute, Vol.16, pp.131-138.
6. Seo, Y-K (2001), "A smooth Elasto-Plastic Cap Model(I): Rate Formulation, Yield Surface Determination", *J. of the KSG*, Vol.17, No.3, pp.15-23.
7. Seo, Y-K (2001), "A smooth Elasto-Plastic Cap Model(II): Integration Algorithm and Tangent Operator", *J. of the KSG*, Vol.17, No.3, pp.25-32.
8. Simo, J. C., Ju, J,-W., Pister, K. S. and Taylor, R. L. (1988), "Assessment of cap model: Consistent return algorithms and rate-dependent extension", *J. Eng. Mech.* 114, pp.191-218.
9. Zaman, M. M., Desai, C. S. and Frauque, M. O. (1982), "An algorithm for determining parameters for cap model from raw laboratory test data", *Proc. 4th Int. Conf. Numer. Meth. Geomech. Edmonton, Canada.*

(received on Mar. 16, 2004, accepted on Apr. 8, 2004)